Elevation Changes in Antarctica Mainly Determined by Accumulation Variability
Michiel M. Helsen, *et al.*
Science **320**, 1626 (2008);
DOI: 10.1126/science.1153894

Elevation Changes in Antarctica Mainly Determined by Accumulation Variability

Michiel M. Helsen,[1]* Michiel R. van den Broeke,[1] Roderik S. W. van de Wal,[1] Willem Jan van de Berg,[1] Erik van Meijgaard,[2] Curt H. Davis,[3] Yonghong Li,[3] Ian Goodwin[4]†

Antarctic Ice Sheet elevation changes, which are used to estimate changes in the mass of the interior regions, are caused by variations in the depth of the firn layer. We quantified the effects of temperature and accumulation variability on firn layer thickness by simulating the 1980–2004 Antarctic firn depth variability. For most of Antarctica, the magnitudes of firn depth changes were comparable to those of observed ice sheet elevation changes. The current satellite observational period (~15 years) is too short to neglect these fluctuations in firn depth when computing recent ice sheet mass changes. The amount of surface lowering in the Amundsen Sea Embayment revealed by satellite radar altimetry (1995–2003) was increased by including firn depth fluctuations, while a large area of the East Antarctic Ice Sheet slowly grew as a result of increased accumulation.

The Antarctic Ice Sheet is constantly adjusting its mass in response to changes in the accumulation of snow on its surface, which occur on centennial to millennial time scales (*1*), with a concomitant effect on global sea level. Although most coupled general circulation models predict the mass of the interior of the Antarctic Ice Sheet to grow in a warmer climate (*2*, *3*), no clear trend has been found there over the past half century (*3*, *4*). On the other hand, extensive areas in coastal Antarctica have recently suffered mass losses through acceleration of coastal glaciers (*5*–*7*). As a result, the latest Intergovernmental Panel on Climate Change assessment estimates a net mass loss of Antarctic grounded ice of 76 ± 127 Gt year^{-1} (1993–2003; 1 Gt = 10^{12} kg), equivalent to 0.21 ± 0.35 mm year^{-1} sea level rise (*8*), with recent estimates showing losses increasing to as much as 196 ± 92 Gt year^{-1} in 2006 (*7*).

One way to estimate ice sheet mass change is through remote measurement of elevation changes (dH/dt) using satellite radar altimetry to determine volume change; this technique has often been applied with an assumption of constant ice sheet density (*9*–*11*). Most studies of the interior of the Antarctic Ice Sheet show extensive areas of slightly increasing elevation, typically by several centimeters per year, suggesting mass gain. However, the unknown depth and density of the firn complicates the conversion from dH/dt to mass change. The densification of firn is influenced by both accumulation rate and temperature, and the thickness of the firn layer therefore varies over time scales of days to millennia (*12*–*14*). Because the period of reliable satellite radar altimetry observations spans only about 15 years, firn depth changes driven by variability in temperature and accumulation may have a large influence on observed elevation trends (*15*). Temperature and accumulation anomalies are correlated in Antarctica and have counteracting effects on firn layer depth: Enhanced accumulation obviously favors firn layer thickening, but as these events coincide with higher than average temperatures, densification in the upper firn pack is enhanced, thus favoring thinning. Previous studies did account for temperature-driven variability of firn compaction (*9*), but in the absence of reliable snowfall time series over the Antarctic Ice Sheet, accumulation rate variability has not been considered in detail.

Here, we derived a corrected dH/dt signal that is free of interannual fluctuations in firn thickness. Our approach combines a firn densification model (*13*) with time series of accumulation and temperature. The firn densification model is forced at the upper boundary with the use of annual accumulation rates from ice cores of various lengths from three Antarctic regions (*16*–*19*), as well as values for skin temperature, solid precipitation, and sublimation from a regional climate model specifically adapted for the Antarctic region (RACMO2/ANT) (*19*, *20*). The regional climate model, in turn, is forced at its lateral boundaries with the use of European Centre for Medium-Range Weather Forecasts (ECMWF) reanalysis (ERA-40) and operational analyses. The forcing with ice core–derived accumulation is used to assess the influence of multidecadal to centennial firn depth variability at the ice core locations, whereas output from the regional climate model (1980–2004) yields interannual firn depth variability over the entire continent.

Relatively modest deviations from the long-term mean accumulation rate can cause large changes in firn depth, especially when the anomalies last for several years (Fig. 1). A critical parameter for our results is this mean accumulation rate that we assume to balance the vertical ice velocity below the firn layer (*19*). We call this the balance accumulation rate (A_b), and its value is estimated using average accumulation rate over the length of the available time series. The shorter the time series, the less valid this approximation is. In theory, the averaging period over which A_b should be calculated is determined by the response time of ice flow to a certain change in accumulation. The response time of an ice mass is inversely proportional to the ice velocity (*21*, *22*), and thus also to A_b. Both velocity (*22*) and A_b (*20*) vary by several orders of magnitude over the Antarctic Ice Sheet. As a consequence, response times vary from millennia (for the dry East Antarctic Plateau) down to several decades (in fast-flowing drainage basins in West Antarctica).

To illustrate the effects of accumulation rate anomalies at different time scales on firn depth variability, Fig. 1B shows simulated firn depth anomalies using a synthetic time series of accumulation rate, keeping annual mean temperature constant (Fig. 1A). Clearly, firn depth changes are determined not by the actual sign of the accumulation trend, but by the period and sign of the accumulation anomaly. In this particular case, a 100-year cycle in accumulation rate dominates the resulting dH/dt pattern. The effect of a 25-year accumulation rate fluctuation is smaller and superimposed on the 100-year signal (Fig. 1B).

Forcing the firn model with accumulation rate time series from an ice core drilled in coastal Dronning Maud Land (DML) (Fig. 1, C and D) reveals that firn depth increased by as much as 4 m between 1850 and 1920, and subsequently fell again by the same amount after 1955, in response to a persisting negative accumulation anomaly. Only in the past two decades does firn depth increase again. In Wilkes Land (WL, using a stack of three ice cores) (*19*), firn depth has been increasing during the past three to four decades because of above-average accumulation rates.

Comparing simulated firn depth time series with linear ice sheet surface elevation trends from the European Remote-Sensing satellite ERS-2 (Fig. 1D) illustrates the limited value of the short satellite time series (1995–2003) in identifying long-term dH/dt values. Simulated firn depth trends at the core sites compare well with ERS-2 dH/dt in DML and in WL, where elevation trends can thus be explained by changes in firn depth. This is not valid for West Antarctica (using a stack of four ice cores) (*19*), where simulated firn depth increases but elevation decreases. This is indicative of dynamic thinning due to the recent acceleration of coastal glaciers (*5*–*7*, *23*).

[1]Institute for Marine and Atmospheric Research, Utrecht University, 3584 CC Utrecht, Netherlands. [2]Royal Netherlands Meteorological Institute, 3732 GK De Bilt, Netherlands. [3]Department of Electrical and Computer Engineering, University of Missouri, Columbia, MO 65211, USA. [4]School of Environmental and Life Sciences, University of Newcastle, Callaghan, NSW 2308, Australia.

*To whom correspondence should be addressed. E-mail: m.m.helsen@uu.nl

†Present address: Climate Risk CoRE and Department of Physical Geography, Macquarie University, NSW 2109, Australia.

As a next step, we applied the firn densification model to the entire grounded Antarctic Ice Sheet over the period 1980–2004, using values of skin temperature, solid precipitation, and sublimation at 6-hour intervals from the regional climate model RACMO2/ANT (*19*, *20*), so that we could correct for all variability < 25 years. For this experiment we used the 1980–2004 average accumulation rate ($A_{80\text{-}04}$) to estimate A_b, and as such we assumed that the ice sheet is in balance with $A_{80\text{-}04}$ (*19*). This period could be far too short to obtain a reliable estimate of A_b. However, ice budget calculations suggest that accumulation and outflow of the East Antarctic Ice Sheet are in near-balance (*7*). A deviation between A_b and $A_{80\text{-}04}$ will be reflected in a difference between simulated firn depth trend and observed dH/dt, and hence is due either to recent change in glacial flow velocity or to changes in accumulation rate on time scales larger than the RACMO2/ANT period.

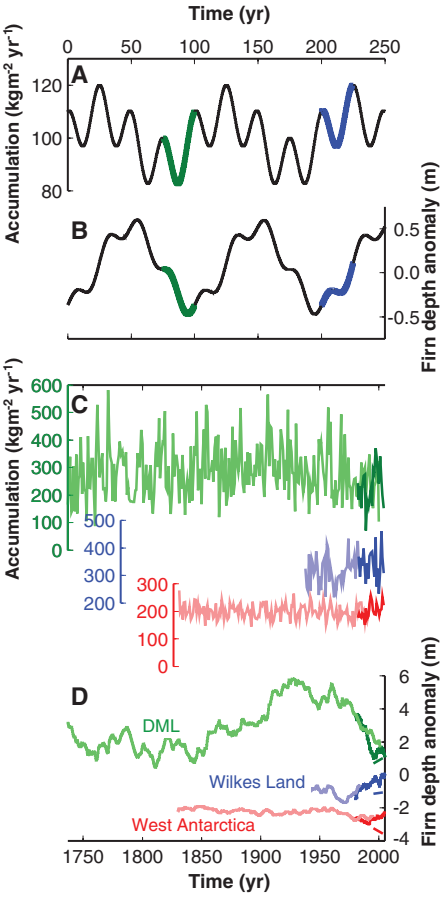

Fig. 1. Simulations of firn depth time series (**B** and **D**) using annual accumulation rate (**A** and **C**) as input data. A synthetic time series of accumulation rate (A) containing sinusoidal fluctuations around A_b = 100 kg m^{-2} year^{-1}, with periodicities of 25 and 100 years and each with an amplitude of 10 kg m^{-2} year^{-1}, results in firn depth changes (B) with a dominant signal on the 100-year time scale. Note the different response of firn depth within two 25-year periods (in green and blue), forced with accumulation time series that are identical in shape but not in their absolute value (A_{green} = 94 kg m^{-2} year^{-1}; A_{blue} = 106 kg m^{-2} year^{-1}). Time series of accumulation rate from ice cores (C) (*16*–*19*) show that irregular deviations from the long-term mean can result in firn depth changes of several meters (D). The light colors in (C) and (D) represent annual accumulation and resulting firn depth records from ice core accumulation data; darker colors are annual accumulation and firn depth records from RACMO2/ANT data (*19*). Observed ERS-2 elevation change trends over 1995–2003 are indicated as straight lines below the simulated firn depth time series; these agree well with firn depth simulations for WL and DML but disagree with West Antarctic firn depth anomalies. Note that the 25-year periods (colored) in (B) are conceptual analogs for the firn depth changes in DML and WL (D). Firn depth changes [in (D)] have been offset by ±2 m for clarity.

In Antarctica, the effect of accumulation rate variability on firn depth by far outweighs the temperature effect (*19*). Consequently, the patterns in simulated firn depth trends over the ERS-2 observational period (1995–2003, Fig. 2A) mainly reflect the 1995–2003 accumulation anomaly (relative to $A_{80\text{-}04}$) (fig. S5). Areas with a positive accumulation anomaly and hence increasing firn depth are found in the Amundsen Sea Embayment (ASE), the Antarctic Peninsula (AP), DML, the Transantarctic Mountains (TM) along the Ross Ice Shelf, and the region east of the Amery Ice Shelf, whereas coastal WL and inland West Antarctica received less than average snowfall, resulting in a decrease in firn depth. The magnitude of simulated firn depth changes (Fig. 2A), –20 to +20 cm year^{-1}, is comparable to satellite-derived dH/dt values (*9*–*11*) (fig. S6). Figure 2A reveals that even during periods of insignificant trends in accumulation rate (*15*), accumulation variability can cause substantial ice sheet elevation changes.

Subtracting simulated firn depth changes (Fig. 2A) from satellite-derived dH/dt (fig. S6) results in an elevation change pattern that is corrected for firn depth variability (dH/dt_{corr}, Fig. 2B). A nonzero value of dH/dt_{corr} indicates an imbalance between $A_{80\text{-}04}$ and vertical ice velocity, but as indicated in Fig. 1, this does not necessarily mean that the ice sheet is out of balance on time scales longer than 25 years. It merely indicates that the 1980–2004 accumulation rate does not accurately represent A_b.

In Fig. 3, the different contributions of elevation change trends are summarized per drainage basin. An extensive error analysis is presented in (*19*). In West Antarctica, a recent positive accumulation anomaly over the ASE and AP has caused increasing firn depths in basins 14 to 19. However, ERS-2 dH/dt observations show a negative dH/dt in the ASE (basins 14 to 16) and in the AP (basin 18). Thus, the firn depth correction enhances the estimate of downward motion relative to the original ERS-2 data (Table 1). This has important implications for the estimation of ice sheet mass changes from dH/dt data (*19*).

The situation for western Palmer Land (PL, drainage basin 17) is different. The simulated firn depths have increased here as well, but they only explain half of the observed increase in surface height. It is likely that the onset of increased accumulation has occurred earlier than 1980, which implies that $A_{80\text{-}04}$ is an overestimate of A_b. This results in a large positive value of dH/dt_{corr} (Fig. 3), in agreement with other reconstructions of accumulation time series from this region (*24*, *25*).

Also in East Antarctica, large differences remain between the 1995–2003 firn depth trends and observed ice sheet elevation changes. In DML (basin 1), when corrected for the fact that firn depth increased during the period 1995–2003, a long-term thinning is found for the multidecadal time scale (Figs. 2B and 3). This is corroborated in Fig. 1D, with firn depth in DML decreasing during the second half the 20th century as the result of a negative accumulation anomaly. The simulated firn depth increase in DML (Fig. 2A) thus represents an overestimate of the observed dH/dt signal, because $A_{80\text{-}04} < A_b$. A conceptual analog for this situation is given by the green lines in Fig. 1, A and B: A negative accumulation anomaly results in a net 25-year negative firn depth trend, while a small elevation increase at the end of the period is visible. Note that these patterns occur without any long-term (<100-year) trend in accumulation.

The opposite situation is found in WL, East Antarctica (basin 6 and 7): Below-average accumulation during 1995–2003 (the satellite period) relative to 1980–2004 (the firn depth model period) causes a decreasing simulated firn depth in Fig. 2A, whereas a positive elevation change is observed. Values of dH/dt_{corr} therefore indicate ice sheet growth, which can be explained if $A_{80\text{-}04} > A_b$. The 25-year analog in Fig. 1, A and B, is outlined by the blue lines; variability within the 25-year period produces both increases and decreases in firn depth, while the dominant signal is a positive firn depth trend, given that the 25-year average accumulation exceeds A_b. Hence, positive dH/dt values in East Antarctica are not caused by a positive trend in accumulation over the period of observation, as suggested by (*10*), but instead by a positive accumulation anomaly over a longer (>25-year) time scale. This also agrees with increased continental average accumulation found for the period 1955–1999 (*3*). These results demonstrate that to confidently assess the mass budget of the Antarctic Ice Sheet from satellite dH/dt data, these observations first need to be further constrained and corrected by a firn densification model forced by independent data (e.g., accumulation time series from ice cores).

We have shown that even insignificant trends in accumulation can cause considerable ice sheet elevation changes. Removing the interannual

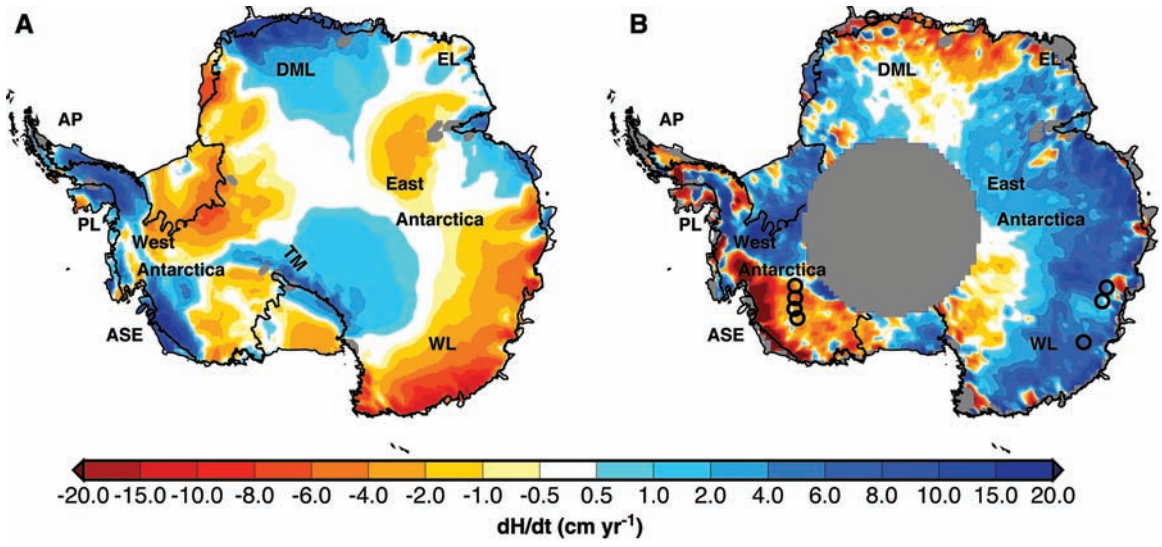

Fig. 2. (**A**) Simulated firn depth trends over the period 1995–2003. (**B**) Observed elevation change trends corrected for firn depth variability as derived from ERS-2 satellite altimetry data over the same period. Firn depth increases over DML, AP, ASE, and along the TM, whereas decreasing firn depths are observed over areas such as WL. The corrected elevation change pattern in (B) reveals a pattern of strongly decreasing ice sheet elevation over the ASE, moderate decreasing elevation over DML, and increasing elevation over a large part of East Antarctica. Black circles in (B) indicate ice core locations that are used in Fig. 1; thick line indicates edge of the grounded ice sheet; gray areas indicate ablation areas (A) and areas without reliable ERS-2 data (B). DML, Dronning Maud Land; EL, Enderby Land; AP, Antarctic Peninsula; PL, Palmer Land; ASE, Amundsen Sea Embayment; TM, Transantarctic Mountains; WL, Wilkes Land.

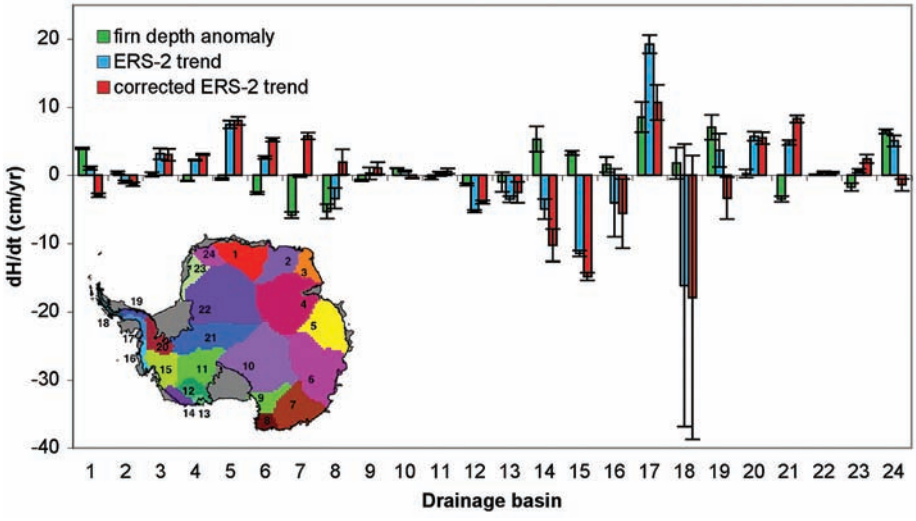

Fig. 3. Surface height changes per drainage basin, with a distinction between contributions of short-term accumulation anomalies (1995–2003 relative to 1980–2004, green bars), the original ERS-2 estimates (1995–2003, blue bars) and the trends computed from ERS-2 data corrected for the 1995–2003 firn depth effects (red bars = blue minus green). Drainage basins 14, 15, and 18 clearly suffer from thinning, whereas drainage basins 5, 6, and 7 in WL evidently show thickening, as does basin 17 in West Antarctica.

Table 1. Elevation changes per area (cm year^{-1}), covering in total 9.4 × 10^6 km^2 (78% of total grounded ice sheet area).

	Firn depth	Uncorrected ERS-2	Corrected ERS-2
ASE	3.5 ± 0.5	−9.2 ± 0.7	−12.7 ± 0.9
Rest of West Antarctica	0.6 ± 0.3	2.1 ± 0.8	1.6 ± 0.8
East Antarctica	−0.6 ± 0.1	1.8 ± 0.5	2.4 ± 0.5
Total	−0.2 ± 0.1	1.1 ± 0.5	1.3 ± 0.5

variability in firn depth from satellite radar altimetry data reveals strong dynamical thinning in the ASE. On the other hand, a large part of the East Antarctic Ice Sheet shows increasing elevation due to accumulation variability on time scales larger than 25 years. We conclude that accumulation variability over a wide range of time scales has a large influence on ice sheet elevation changes, and needs to be taken into account for the assessment of the Antarctic mass budget.

References and Notes

1. J. Oerlemans, *Nature* **290**, 770 (1981).
2. G. A. Meehl *et al.*, in *Climate Change 2007: The Physical Science Basis*, S. Solomon *et al.*, Eds. (Cambridge Univ. Press, Cambridge, 2007), pp. 747–845.
3. A. J. Monaghan, D. H. Bromwich, D. P. Schneider, *Geophys. Res. Lett.* **35**, L07502 (2008).
4. A. J. Monaghan *et al.*, *Science* **313**, 827 (2006).
5. E. Rignot, R. H. Thomas, *Science* **297**, 1502 (2002).
6. R. H. Thomas *et al.*, *Science* **306**, 255 (2004); published online 23 September 2004 (10.1126/science.1099650).
7. E. Rignot *et al.*, *Nat. Geosci.* **1**, 106 (2008).
8. P. Lemke *et al.*, in *Climate Change 2007: The Physical Science Basis*, S. Solomon *et al.*, Eds. (Cambridge Univ. Press, Cambridge, 2007), pp. 337–383.
9. H. J. Zwally *et al.*, *J. Glaciol.* **51**, 509 (2005).
10. C. H. Davis, Y. Li, J. R. McConnell, M. M. Frey, E. Hanna, *Science* **308**, 1898 (2005); published online 19 May 2005 (10.1126/science.1110662).
11. D. J. Wingham, A. Shepherd, A. Muir, G. J. Marshall, *Philos. Trans. R. Soc. London Ser. A* **364**, 1627 (2006).
12. R. J. Arthern, D. J. Wingham, *Clim. Change* **40**, 605 (1998).
13. H. J. Zwally, J. Li, *J. Glaciol.* **48**, 199 (2002).
14. J. Li, H. J. Zwally, J. C. Comiso, *Ann. Glaciol.* **46**, 8 (2007).
15. M. R. van den Broeke, W. J. van den Berg, E. van Meijgaard, *Geophys. Res. Lett.* **33**, L02505 (2006).
16. I. Goodwin, M. de Angelis, M. Pook, N. W. Young, *J. Geophys. Res.* **108**, 10.1029/2002JD002995 (2003).
17. M. Kaczmarska *et al.*, *Ann. Glaciol.* **39**, 339 (2004).
18. S. Kaspari *et al.*, *Ann. Glaciol.* **39**, 585 (2004).
19. See supporting material on *Science* Online.
20. W. J. van de Berg, M. R. van den Broeke, C. H. Reijmer, E. van Meijgaard, *J. Geophys. Res.* **111**, D11104 (2006).
21. J. F. Nye, *Geophys. J. R. Astron. Soc.* **7**, 431 (1963).
22. J. L. Bamber, D. G. Vaughan, I. Joughin, *Science* **287**, 1248 (2000).
23. A. Shepherd, D. J. Wingham, J. A. D. Mansley, H. F. J. Corr, *Science* **291**, 862 (2001).
24. J. Turner, T. Lachlan-Cope, S. Colwell, G. J. Marshall, *Ann. Glaciol.* **41**, 85 (2005).
25. E. R. Thomas, G. J. Marshall, J. R. McConnell, *Geophys. Res. Lett.* **35**, L01706 (2008).

26. We thank M. Kaczmarska, S. Kaspari, and A. Monaghan for generously providing time series of accumulation rates, and three anonymous reviewers for their comments

that improved this manuscript. Supported by NWO's Netherlands Polar Programme (M.M.H., W.J.v.d.B.) and by NASA's Cryospheric Sciences Program (C.H.D., Y.L.). ERS-2 radar altimeter data were provided by NASA Goddard Space Flight Center. All authors have discussed results and contributed to the manuscript. M.M.H. developed the firn densification model, and integrated the results. M.M.H., M.R.v.d.B., and R.S.W.v.d.W. frequently discussed results. M.R.v.d.B., W.J.v.d.B., and E.v.M. contributed to RACMO2/ANT data. C.H.D. and Y.L. analyzed elevation changes from ERS-2 data. I.G. contributed to accumulation records.

Supporting Online Material
www.sciencemag.org/cgi/content/full/1153894/DC1
Materials and Methods
Figs. S1 to S9
Table S1
References

7 December 2007; accepted 7 May 2008
Published online 29 May 2008;
10.1126/science.1153894
Include this information when citing this paper.

Natural Selection Shapes Genome-Wide Patterns of Copy-Number Polymorphism in *Drosophila melanogaster*

J. J. Emerson,[1,2]*† Margarida Cardoso-Moreira,[1,3,4]*† Justin O. Borevitz,[1] Manyuan Long[1]

The role that natural selection plays in governing the locations and early evolution of copy-number mutations remains largely unexplored. We used high-density full-genome tiling arrays to create a fine-scale genomic map of copy-number polymorphisms (CNPs) in *Drosophila melanogaster*. We inferred a total of 2658 independent CNPs, 56% of which overlap genes. These include CNPs that are likely to be under positive selection, most notably high-frequency duplications encompassing toxin-response genes. The locations and frequencies of CNPs are strongly shaped by purifying selection, with deletions under stronger purifying selection than duplications. Among duplications, those overlapping exons or introns, as well as those falling on the X chromosome, seem to be subject to stronger purifying selection.

Differences in the numbers of copies of large DNA segments are an abundant source of genetic variation in humans (*1*, *2*), mice (*3*), and flies (*4*). Because CNPs can create new genes, change gene dosage, reshape gene structures, and/or modify the elements that regulate gene expression, understanding their evolution is at the very heart of understanding how such structural changes in the genome contribute to the phenotypic evolution of organisms (*5*–*7*).

A rigorous characterization of CNPs requires high-resolution data unbiased with respect to genome annotation. We used tiling arrays covering the full euchromatic genome of *D. melanogaster* at a median density of one unique perfect match probe for every 36 base pairs (bp) (*8*, *9*) in 15 natural isofemale lines (table S1). We inferred copy-number changes with a hidden Markov model (HMM) (*9*) that inferred the posterior probabilities for copy number by comparing DNA hybridization intensities between natural isolates and the reference genome strain. Training data for copy-number changes were obtained via hybridization with a line known to contain a ~200-kb homozygous duplication and from a set of 52 validated homozygous deletions (*9*). The probabilities of mutation were parsed to make CNP calls (table S3).

Because tiling arrays are restricted to nonredundant regions in the reference genome, deletion and duplication are detected by the absence of nonredundant DNA and by the doubling of unique DNA, respectively. In principle, it is possible to confound unique duplications with multiple hit scenarios of deletion of ancestral duplications. However, the few CNPs that exhibited even weak signs of ancestral redundancy in either *D. simulans* or *D. yakuba* (109 CNPs) showed a site-frequency spectrum (SFS) suggesting that the derived state cannot be a deletion [table S4; (*9*)]. Nevertheless, we excluded those events from our analyses.

In order to validate the CNP predictions, we performed polymerase chain reaction–based assays (*9*). For duplications, we obtained a false-positive rate of 14% and a false-negative rate of 16%. Notably, our assay can only amplify tandem duplications lying within several kilobases of each other, suggesting that the false-positive rate is overestimated. Conversely, the fact that we confirmed 86% of the duplications confirms that most CNPs form in tandem. For deletions, we obtained a false-positive rate of 47%. This high rate of falsely called deletions is in part due to the prevalence of multiple adjacent single-nucleotide polymorphisms (SNPs) in highly polymorphic regions of the *D. melanogaster* genome (*10*). We also obtained a false-negative rate of 18% for homozygous deletions and 32% for heterozygous deletions.

We detected 2658 unique CNPs among all 15 lines of *D. melanogaster*, with an average of 312 CNPs (SD = 31.9 CNPs), after adjusting for false positives. Except where noted, total mutation counts are corrected only for false positives. In total, CNPs comprise ~2% of the genome. The size distribution of CNPs was roughly exponential, with most being small variants (median: 336 bp) and few being larger variants (maximum size detected: 35 kb). The predicted and real CNP boundaries differ only by about one probe for duplications and about three probes for deletions (table S3). These data indicate that we were able to both detect

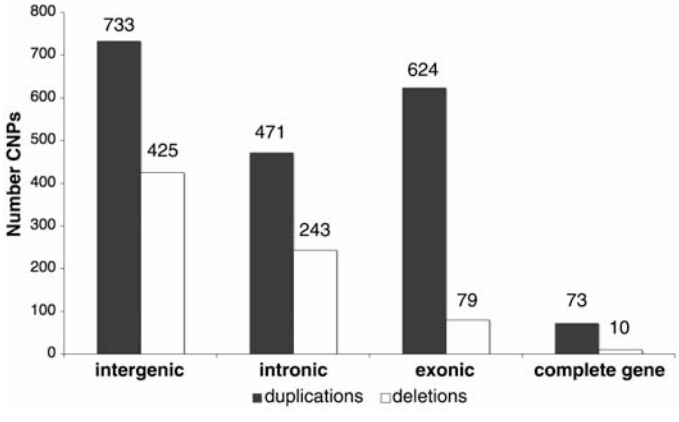

Fig. 1. Frequency of CNPs within different genomic contexts. The numbers of polymorphic duplications (black) and deletions (white) are shown for four mutually exclusive genomic contexts: intergenic (mutations between genes), intronic (mutations entirely within introns), exonic (mutations that overlap exons but not complete gene structures), and complete gene (mutations that overlap at least one complete gene structure, including UTRs).

[1]Department of Ecology and Evolution, University of Chicago, Chicago, IL 60637, USA. [2]Genomics Research Center, Academia Sinica, Taipei 115, Taiwan. [3]Graduate Program in Areas of Basic and Applied Biology, Universidade do Porto, Porto, Portugal. [4]Faculdade de Ciências, Universidade do Porto, Porto, Portugal.

*These authors contributed equally to this work.
†To whom correspondence should be addressed. E-mail: jje@uchicago.edu (J.J.E.); mmoreira@uchicago.edu (M.C.M.)